XII. BEAM-GLOBAL CORRELATIONS

In the last two sections correlations between diffuse and global radiation were discussed. For many solar energy systems information about the direct beam component of solar radiation is more valuable. This is particularly the case for applications that concentrate incident energy to attain the high thermodynamic efficiency achievable only at higher temperatures. In order to evaluate the performance of concentrating systems it is necessary to know the intensity of the beam radiation, as only this component can be concentrated.

While there are numerous locations around the world where global irradiance has been monitored, continuous records of the beam component are scarce. The limited amount of direct beam monitoring is undoubtedly due to the constant care necessary in gathering and analyzing the data. Often the beam component has to be estimated using an empirical correlation procedure. Historically, the most common method has been to use a three phase approach. First the correlation between diffuse and global solar radiation is used to determine the diffuse component on a horizontal surface [1-5]. Then the direct component on the horizontal surface could be obtained by subtraction, and finally the beam radiation is approximated by a calculational procedure. A more straightforward and accurate approach is to calculate the beam radiation directly using a beam-global correlation.

At first glance it would seem that the two correlations are related since on an instantaneous basis the direct component on the horizontal surface (easily obtainable from the diffuse-global correlation) is equal to the beam irradiance multiplied by the cosine of the incident angle. For hourly values the beam energy can be calculated with reasonable accuracy by dividing the hourly average horizontal direct value by the average of the cosine over that hour. However, if this method is applied to daily data, a systematic error results due to considerable atmospheric attenuation during the morning and evening hours. This affect is not taken into account by the simple averaging procedure [6]. While it is possible to remove this error by properly weighing the cosine over the day, it is simpler and more precise to use a correlation between the beam and global values.

Prior to 1986, little had been published on beam-global correlations. Randall and Whitson [7] have obtained an hourly beam-global correlation derived from data measured at several sites, but do not give daily or monthly correlations. A more recent paper [8] presents nine years of beam and global data for Bet Dagan, Israel on an hourly, daily, monthly, and yearly basis without presenting the regression fits. In this section we present results on daily and monthly beam-global correlations obtained from data gathered through 1984 from seven solar radiation monitoring sites in the Pacific Northwest. A more extensive study can be found in **Solar Energy** [9].

The discussion is organized as follows. First the procedures used to derive the correlations are described along with the correlation results. As with the diffuse-global correlations presented in the previous sections, the beam-global correlations exhibit a pronounced seasonal variation. A simple analytic method is demonstrated which emulates this seasonal variation and is used to better describe the data. The effect of the eruption of El Chichón on the correlations is also discussed. Finally, the usefulness of the correlations is discussed and a summary of important results is presented.

Method of Analysis

Data for this analysis come from seven first class sites in the Pacific Northwest. Six of the sites are part of the UO Solar Monitoring Network; the other is the Solar Energy Meteorological Research and Training Site (SEMRTS)

in Corvallis. The SEMRTS data serves as an excellent independent check on our results.

The first step prior to starting the correlation process was to normalize the daily beam and global data. Beam values were divided by extraterrestrial radiation giving K_B and global values were divided by extraterrestrial radiation on a horizontal surface giving the clearness index K_T. The value of the solar constant used in this study was 1370 W/m^2. Beam values were correlated directly with global values unlike the diffuse-global correlation in which diffuse values were first divided by global values. Plots of the normalized daily and monthly averaged data are shown in Figs. 35 and 36.

Daily correlations were derived using standard regression procedures. The monthly averaged correlations were obtained using a moving average approach discussed in section X to make more complete use of the data.

Correlation Results

Daily and monthly averaged beam-global correlations were obtained for each of the seven first class sites in Oregon and Idaho. Correlations were also derived using the combined data from all sites. The data for the daily values were best described by a correlation with a cubic dependence on K_T. A dependence on higher order terms in K_T was found to be statistically insignificant. For monthly averaged values a quadratic dependence on $\overline{K}_T$ was sufficient to describe the data sets. Regression coefficients are listed in Tables 15 and 16.

The use of a cubic fit for the daily correlations results in a regression curve that has a minimum at $K_T \cong 0.15$. This is an artifact of the correlation procedure and does not represent the behavior of the data. To eliminate this false minimum, the few data points with K_T below 0.15 were fit separately. The best overall fit is given in Table 15.

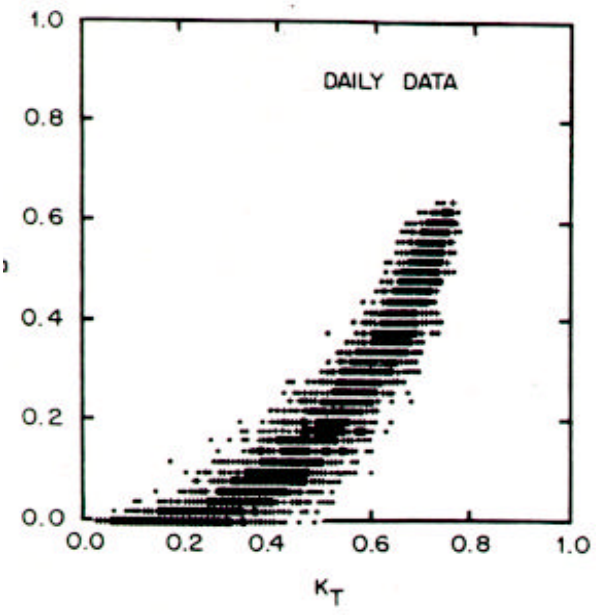

Fig. 35: Daily correlation data for all seven PNW stations. The large, solid circles (•) show the region of highest density, the crosses (+) indicate a region of lower density, and the small, solid circles (·) indicate one or two data points.

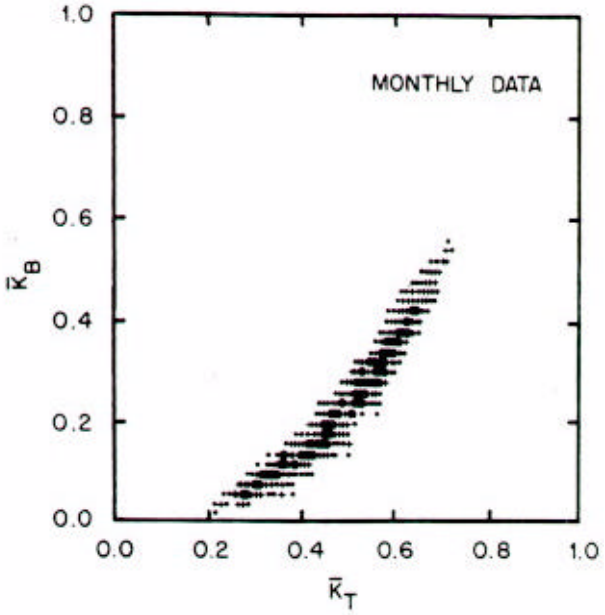

Fig. 36: Monthly correlation data for all seven PNW stations. The symbols are used to indicate the density of values as described in the caption of Fig. 35.

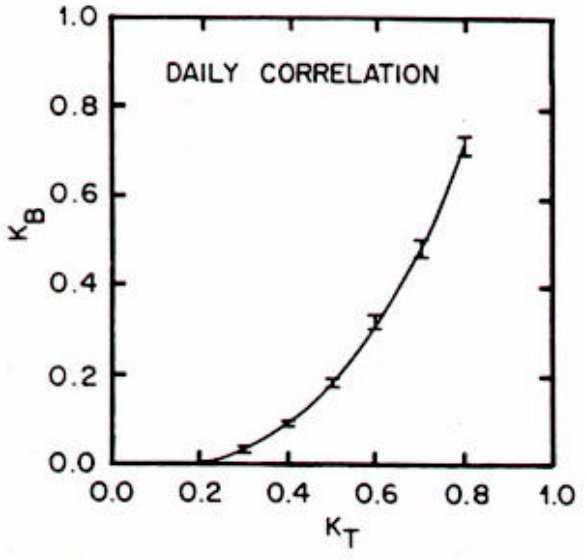

Fig. 37: Daily regression curve for combined data set. The bars indicate the maximum spread the regression fits.

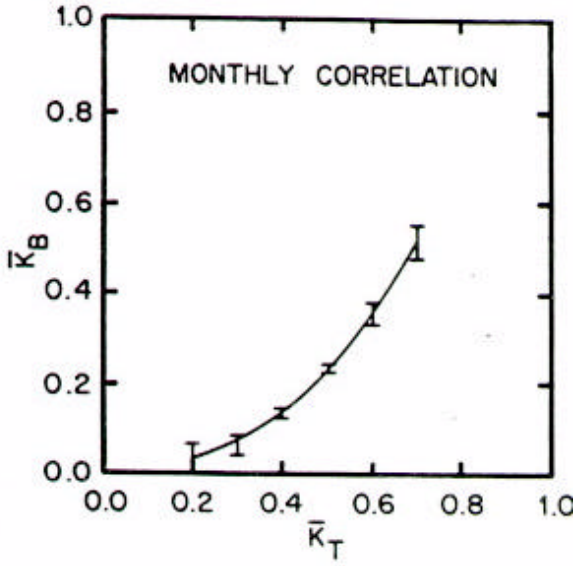

Fig. 38: Monthly regression curve for combined data set. The bars indicate the maximum of spread of the regression fits.

Plots of the daily and monthly average regression curves for all sites are shown in Figs. 37 and 38 respectively. The plots for specific sites were not included because they fall so close together. Instead, vertical bars show the maximum difference between the correlations on the graphs. The spread between the monthly correlations is greater than for the daily correlation partially due to the lack of data at extreme values of $\overline{K}_T$. In the region between $\overline{K}_T$ of 0.4 and 0.5 all the correlations agree to better than 5% with the average correlation.

A comparison between daily, 10 day and monthly averaged regression fits is shown in Fig. 39. This is similar to results obtained for diffuse-global correlations where regression curves derived from data averaged over 5 to 30 days were almost identical. The daily regression curve falls considerably below the monthly curve. For high values of K_T the curves merge as would be expected if the month had all clear days.

When the correlation analysis is performed, a regression curve, which fits the average value of the data, is obtained along with information about the variance of the data about mean. The residual standard deviation as a percent of the mean (%σ) is indicative of the scatter of the data points about the regression curve. The factor R^2, also given in the tables, measures the portion of total variation about the mean explained by the regression analysis.

An examination of the distribution of the data about the regression curve is helpful in determining how well the correlation describes the

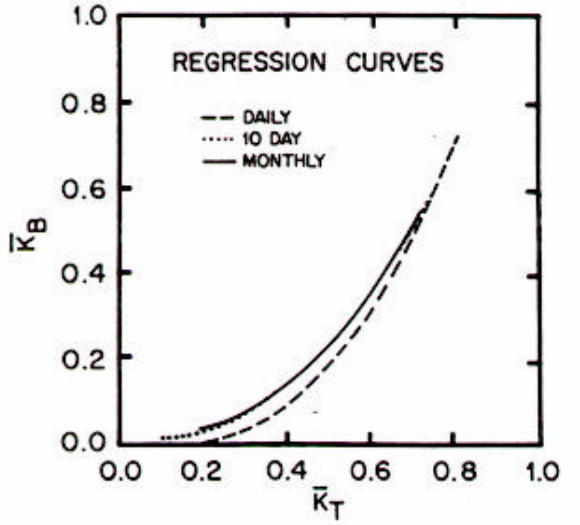

Fig. 39: Regression curves for daily, 10 day, and monthly correlations. Notice that the 10-day and the monthly regression curves overlap.

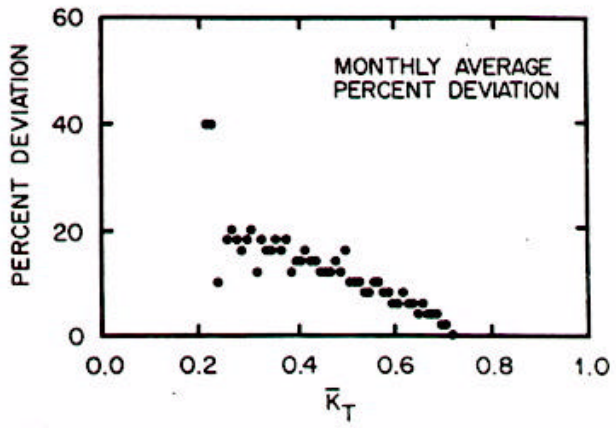

Fig. 40: Percent standard deviation for monthly correlations plotted against $\bar{K}_T$.

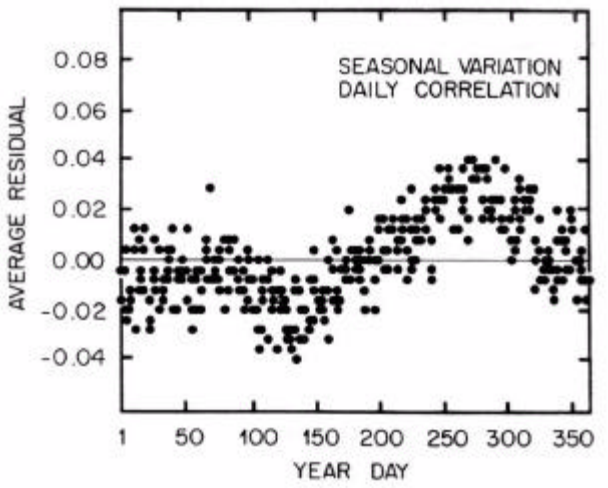

Fig. 41: Average residuals for the daily correlations plotted against time of year.

data. For example, the percent deviation as a function of $\bar{K}_T$ is plotted for monthly data in Fig. 40. Notice that the percent deviation decreases by a factor of 10 as $\bar{K}_T$ increases to its maximum value. This means that on a percentage basis the more clear days, the more precise the beam value can be determined from the global data. The same holds true for daily values.

Seasonal Variations

Dependence of the correlation on other variables can be seen by plotting the residuals against those variables. When residuals are plotted against time of year, as in Fig. 41, the dependence on year-day becomes evident. This is the same seasonal dependence as was found for diffuse-global correlations. Terms involving the sine of the year-day were used to emulate this variation for the diffuse-global correlations and similar terms work here to improve the beam-global correlations. For the monthly average case $\bar{K}_T$ multiplied by the sine term gave the best improvement. The equation used for the seasonally adjusted monthly correlation is

$$\bar{K}_B = a + b\cdot\bar{K}_T + c\cdot\bar{K}_T^2 + d\cdot\bar{K}_T\cdot\sin(2\pi(N-2)/365) \quad (1)$$

where the year-day (N) is in the middle of the 30 day period.

For the daily correlation, both K_T and K_T^2 times the sine term are statistically significant. The formula used for the seasonally adjusted daily correlation is

$$K_B=a+b\cdot K_T+c\cdot K_T^2+d\cdot K_T^3+(e\cdot K_T+f\cdot K_T^2)\cdot\sin(2\pi(N-20)/365) \quad (2)$$

where N is the year-day under consideration.

Tables 15 and 16 contain the regression fits for the daily and monthly averaged data. Regression curves derived from correlations including the sine terms do not differ much from regression curves without the sine terms because the seasonal variations average out over the year. The improvement manifests itself in a reduction of the standard deviation. For monthly correlations the standard deviation is reduced by about 20% while for daily correlations the reduction is 8%. The sine terms account for most of the seasonal variance in the data. It turns out that the reduction in standard deviation is much greater for clear days than for cloudy days. If one is modeling clear days inclusion of the seasonal variation sine terms can significantly improve the results.

Effect of El Chichón

In the previous section on diffuse-global correlations, the seasonal variation was connected with changes in water vapor, turbidity, and air mass. Prior to the eruption of El Chichón both

Table 15. Daily Regression Fits[†]

All Sites	A	b	C	d	e	f	ϕ°	%σ	R^2
All Data (no sine)	0.022	-0.280	0.828	0.765	----	----	--	17.4	95.3
All Data (sine)	0.013	-0.175	0.520	1.030	0.038	-0.130	-20	16.1	96.8
Before April 1982	0.014	-0.175	0.508	1.077	0.057	-0.170	-40	15.6	96.2
After April 1982	0.013	-0.171	0.535	0.945	-0.025	-0.030	+20	16.0	96.0

[†]*For K_T<0.175 For fits with no sine term $K_B = 0.016.K_T$.*
For fits with sine terms $K_B = 0.125.K_T^2$.

Table 16. Monthly Average Regression Fits

All Stations	a	B	C	d	ϕ°	%σ	R^2
All Data (no sine)	0.051	-0.356	1.449	----	---	9.4	96.1
All Data (sine)	0.004	-0.150	1.240	-0.038	-20	7.7	97.4
Before April 1982	0.003	-0.161	1.283	-0.046	-40	7.3	97.9
After April 1982	-0.008	-0.062	1.083	-0.043	+20	6.7	97.7

the phase of the sine term and the magnitude of the coefficients in the beam-global correlations compared well with what one would estimate from the diffuse-global correlations.

Since the eruption, the phase (ϕ) of the sine term has changed slightly from the phase in the previous section. During April 1982 El Chichón ejected considerable material into the upper atmosphere. These aerosol particles have periodically reduced the beam component during the last few years in the Pacific Northwest. In section IX, it was shown that the effect on global radiation was minor compared to the change in the beam component. This difference caused the shift in the phase of the sine term.

Correlations derived with data before the eruption of El Chichón are different than those derived with data obtained after the eruption. The daily and the monthly regression fits before and after the eruption are given in Tables 15 and 16. The magnitude of the beam values calculated for high values of K_T before the eruption are a few percent higher than for the values after the eruption. The change in correlation coefficients are the result of the large reduction in beam radiation as compared to global radiation during the winter months caused by scattering from the volcanic aerosol cloud. The shift in volcanic aerosol cloud. The shift in phase of the sine terms is caused by the seasonal appearance of the volcanic cloud. Reference [10] contains a more extensive description of the effects of the eruption of El Chichón on correlations with global radiation.

Conclusions

Good beam and global data are essential to accurately estimate of the performance of solar energy systems. Usually only global data are available and it is necessary to calculate the beam energy. A good approximation of the beam values can be obtained from the correlations presented in this section. On average, the beam energy on individual days can be determined to within 20% of the actual value while monthly averages can be determined to within 10%. This percent accuracy is not a precise measure as it is a steep function of the clearness index K_T. Values on clear days can be estimated with a considerably higher precision. On a long term average basis the average annual uncertainty introduced by using the correlations is small, on the order of several percent. This is even true for many sites outside the Pacific Northwest. Therefore, while these correlations cannot replace good data, they can be used to

generate beam values that imitate the actual data.

No significant difference was found between the beam global correlations for the seven sites used in this study even though they represent diverse climatalogical regions. The difference between the correlations was further reduced when the seasonal dependence of the data is taken into account. Sine terms, dependent only on the day of the year, were used to simulate this seasonal variation and their use significantly improves the correlations.

The relevance of these correlations for regions outside the Pacific Northwest has been tested at a limited number of sites. For the NOAA sites examined, the correlations appear satisfactory. The use of the PNW seasonal variation regression terms improved the fit to the data. The data from Bet Dagan, Israel does not appear to match the present regression curves at high values of K_T, where the difference can reach 10 to 20 percent. The difference in turbidity between the two regions is the suspected cause of the difference. Clearly more data from a number of sites is needed to better test the general applicability of the PNW correlations.

The accuracy to which beam values can be determined from correlations is highly dependent on the precision of the global measurements. Any error in the global data translates into twice the error for the calculated beam value because to a close approximation the beam value is proportional to the square of the global value. This problem is particularly severe with global data collected with second class pyranometers that tend to exhibit systematic errors that vary with time of year [11]. The validity of beam values becomes much more uncertain when they are derived from global values calculated from meteorological models.

The difference between correlations before and after the eruption of El Chichón demonstrates that global correlations are indeed dependent on turbidity. The magnitude of the change in the relationship between beam and global radiation is proportional to the change in transmission values. Normal changes in turbidity and other atmospheric components over the year also effect the correlations about as much as they effect transmission values.

Accounting for the seasonal variation due to changes in atmospheric constituents a subtle but significant improvement to the correlations. Only high quality data allows one to observe the effects of changes in air mass, turbidity, and water vapor. Inclusion of these atmospheric effects through the seasonal variation term accounts for some of the data's variance and allows for a more accurate determination of the beam value, especially on clear days.

The difference between correlations before and after the eruption of El Chichón demonstrates that global correlations are indeed dependent on turbidity.

While hourly diffuse-global correlation can be used to accurately estimate hourly beam values, extrapolation of this procedure to daily or monthly averaged data leads to serious errors. This can be seen in figures from reference [8] where they used the diffuse-global correlations of reference [2] to estimate beam values to compare with their data. For hourly values the two curves match very closely, but for daily and monthly averaged results the curves differ by about 15 to 20 percent because only a simple average of the cosine was used to estimate the beam value. Reference [6] studies this problem in detail.

References

1. B. Y. H. Liu and R. C. Jordan, The Interrelationship and Characteristic Distribution of Direct, Diffuse and Total Solar Radiation. **SOLAR ENERGY** 4, 1-19 (1960).

2. A. Collares-Pereira and A. Rabl, The Average Distribution of Solar Radiation-Correlations Between Diffuse and Hemispherical and Daily and Hourly Insolation Values**. SOLAR ENERGY** 22, 155-164 (1979).

3. D. G. Erbs, S. A. Klein and J. A. Duffie, Estimation of the Diffuse Radiation Fraction for Hourly, Daily, and Monthly- Averaged Global Radiation. **SOLAR ENERGY** 28, 293-302 (1982).

4. F. Vignola and D. K. McDaniels, Correlations Between Diffuse and Global Insolation for the Pacific Northwest. **SOLAR ENERGY** 32, 161-168 (1984).

5. F. Vignola and D. K. McDaniels, Diffuse-Global Correlations: Seasonal Variations **SOLAR ENERGY** 33, 397-402 (1984).

6. F. Vignola and D. K. McDaniels, Transformation of Direct Solar Radiation to Tilted Surfaces. **Proceedings of the 1984 Annual Meeting American Solar Energy Society, Inc**., Anaheim, Calif., 651-655 (1984).

7. C. M. Randall and M. E. Whitson Jr., Hourly Insolation and Meteorological Data Bases Including Improved Direct Insolation Estimates. Aerospace Report No ATR-78(7592)-1.

8. J. M. Gordon and M. Hochman, On Correlations Between Beam and Global Radiation. **SOLAR ENERGY** 32, 329-336 (1984).

9. F. Vignola and D. K. McDaniels, Beam-Global Correlations in the Pacific Northwest. **SOLAR ENERGY** 36, 409-418 (1986).

10. F. Vignola and D. K. McDaniels, Effects of El Chichón on Global Correlations. **Proceedings of the Ninth Biennial Congress of the International Solar Energy Society**. Montreal, Canada, 2434-2438 (1985).

11. Edwin C. Flowers**, Solar Radiation Facility – Report for 1978**. NOAA/ERL-ARL, Boulder, CO.